THE BELL SYSTEM
TECHNICAL JOURNAL

VOLUME XLI MARCH 1962 NUMBER 2

Resistivity of Bulk Silicon and of Diffused Layers in Silicon

By JOHN C. IRVIN

(Manuscript received July 25, 1961)

Measurements of resistivity and impurity concentration in heavily doped silicon are reported. These and previously published data are incorporated in a graph showing the resistivity (at $T = 300°K$) of n- and p-type silicon as a function of donor or acceptor concentration.

The relationship between surface concentration and average conductivity of diffused layers in silicon has been calculated for Gaussian and complementary error function distributions. The results are shown graphically. Similar calculations for subsurface layers, such as a transistor base region, are also given.

I. INTRODUCTION

A diffused layer in silicon is generally characterized by four parameters: the concentration, C_s, of diffused donors or acceptors at the surface, the concentration, C_B, of acceptors or donors originally in the material (background concentration), the depth, x_j, of the resultant junction, and the sheet resistivity, ρ_s, of the layer. A knowledge of the relationship between these parameters is essential to the establishment of device processing recipes, the evaluation of diffusion techniques, and investigations of the thermodynamic properties of silicon.

The desired relationship may be readily calculated, given a knowledge of the distribution of the diffused impurities, the variation of the resistivity of n- and p-type silicon with donor or acceptor density, and a fast electronic computer. The results of such a computation were first

made generally available three years ago, in the form of curves relating C_s to $1/\rho_s x_j$ for a given C_B, for n- and for p-type layers in silicon, and for several common distributions.[1] Recent calculations, however, based on new and more extensive silicon resistivity data, have indicated considerable error in the earlier results. Thus a comprehensive recomputation has been undertaken, the outcome of which is presented herewith.

A necessary adjunct to the calculation is an accurate knowledge of the resistivity of n- and p-type silicon with varying dopant concentration. To this end, most of the extant data have been reviewed and supplemented here and there with some new determinations. The results of this search are also presented here.

II. THE RESISTIVITY OF SILICON AS A FUNCTION OF IMPURITY CONCENTRATION

The variation of the resistivity of silicon at 300°K as a function of the concentration of acceptors or donors is shown in Fig. 1. This graph represents the author's judgment of a most reasonable compromise to

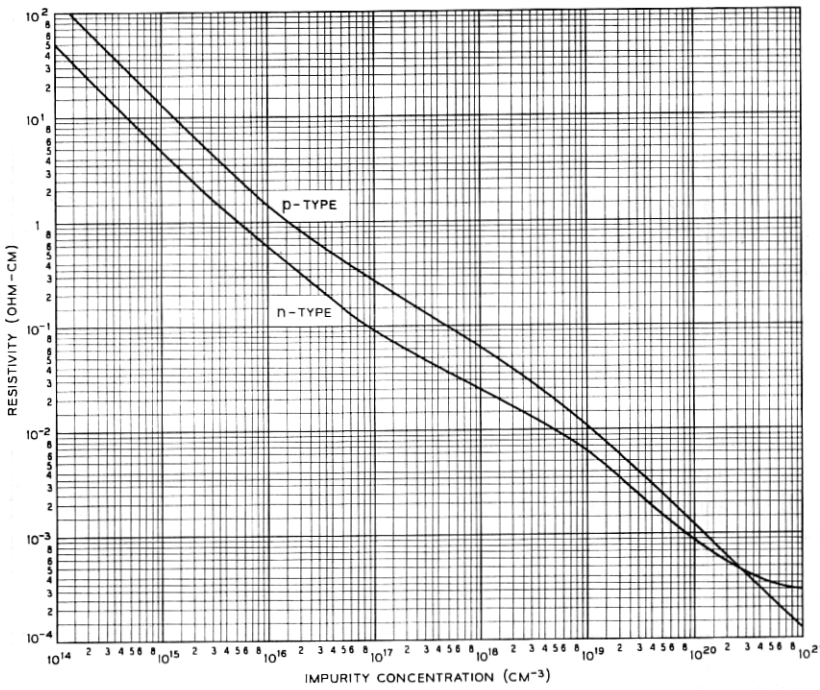

Fig. 1 — Resistivity of silicon at 300°K as a function of acceptor or donor concentration.

TABLE I — RESISTIVITIES AND IMPURITY CONCENTRATIONS IN SILICON (T = 300°K)

Resistivity (ohm-cm)	Impurity	Impurity Concentration (cm^{-3})	Carrier Concentration (cm^{-3})
0.00076	B	1.66×10^{20}	
0.00089	B	1.41×10^{20}	
0.0010	B		1.49×10^{20}
0.0010	B	1.12×10^{20}	
0.0012	B	1.04×10^{20}	
0.0011	B	1.12×10^{20}	
0.0014	B	9.23×10^{19}	
0.0013	B	8.84×10^{19}	
0.0067	B	1.43×10^{19}	
0.0073	B	1.43×10^{19}	
0.013	B	7.41×10^{18}	
0.014	B	7.03×10^{18}	
0.00095	As	1.80×10^{20}	
0.00094	As	1.86×10^{20}	
0.00094	As		1.1×10^{20}
0.00093	As	1.87×10^{20}	
0.00094	As	1.97×10^{20}	
0.00088	As	2.10×10^{20}	
0.00088	As	2.19×10^{20}	
0.00089	As		1.1×10^{20}
0.00083	As	2.30×10^{20}	
0.00083	As	2.20×10^{20}	
0.00080	As	2.46×10^{20}	
0.00082	As	2.44×10^{20}	

the mass of available and not altogether compatible data on the subject. These data include most of the previously published work (Refs. 3–12), recent, unpublished results kindly provided by other investigators,[2,13] as well as some measurements obtained expressly for the present study.

The last data are shown in Table I. The crystals involved were pulled from quartz crucibles, and hence can not be expected to be particularly low in oxygen content. After dissolution of the boron-doped crystals and separation of the dopant,[14] boron concentrations were determined by a photometric carmine technique essentially similar to published methods.[15] Arsenic concentrations were measured by gamma-ray spectrometry after pile neutron activation. Resistivity measurements were done with a four-point probe. In the case of a few samples, resistivity and carrier concentration were measured in Hall-effect apparatus (where it was assumed $\mu_H/\mu = 1$).

Drawing curves through these many points was accomplished by a succession of smoothing procedures, which were primarily visual. 75 per cent of the data points deviate less than 10 per cent from the curves thus obtained, both for the p-type and the n-type cases. The uncertainty is greatest in the degenerate region. For p-type silicon, suitable data be-

come scarce at dopings greater than 10^{19} cm^{-3}, and none are available beyond 3×10^{20} cm^{-3}. For n-type material, there is an abundance of rather conflicting data representing donor concentrations between 10^{19} cm^{-3} and 6×10^{20} cm^{-3}. In this region a 10 per cent variation in the chosen line still includes 67 per cent of the data, however.

A single pair of curves obviously can not characterize with the same degree of accuracy all silicon material, regardless of dopant employed or degree of compensation. However, over the range 10^{14} cm$^{-3} \leqq N_I \leqq 10^{20}$ cm^{-3}, and subject to the limitations discussed below, Fig. 1 is considered to be within 10 per cent of reality. This graph refers specifically to uncompensated silicon containing a donor or acceptor impurity concentration, N_I, consisting of arsenic, phosphorus, or antimony for n-type, and aluminum, boron, or gallium for p-type material. (Actually, even among samples doped with the aforementioned impurities, small but consistent differences in carrier concentration and mobility, depending on the specific choice of donor or of acceptor, have been reported recently for silicon in the 0.001 ohm-cm region.[10,12]) In case of moderate compensation, the net impurity density, $|N_A - N_D|$, should be used for N_I. However, heavy compensation requires allowance for the added impurity scattering.

For impurity densities near or greater than 10^{20} cm^{-3}, Fig. 1 can not be considered very reliable. At such concentrations, impurity band conduction is prominent and its effects are apt to differ appreciably depending on choice of impurity. Even more serious are the degrees of impurity precipitation and lattice imperfection which occur in highly doped material and which furthermore vary with growth conditions and history of the crystal. It will be noted with some consternation that the p-type and n-type curves are shown to cross near $N_I = 3 \times 10^{20}$ cm^{-3}. The paucity of data, of course, casts considerable doubt on this result. However, for what they are worth, such are the indications. Perhaps this can be understood in light of the acceptor action of imperfections, especially vacancies, which are abundant in very highly doped material.

The calculations discussed in the remainder of this paper require a mathematical representation of Fig. 1. Straight-line approximations of the form $(1/\rho) = BN_I^{\alpha}$ have been obtained, which depart 10 per cent from the desired curve at the turning points and rapidly approach coincidence elsewhere. The parameters B and α are listed in Table II for the respective straight-line regions.

III. DIFFUSION PROFILES AND CALCULATIONS

The diffusion profiles of current practical interest are the complementary error function, $C_x = C_s \operatorname{erfc} (x/2\sqrt{Dt})$, and the Gaussian,

TABLE II — VALUES OF B AND α IN THE EQUATION $(1/\rho) = BN_I^{\alpha}$, REPRESENTING STRAIGHT-LINE APPROXIMATIONS TO THE ρ VS N_I CURVES OF n-TYPE AND p-TYPE SILICON (T = 300°K)

Region (cm^{-3})	B	α
n-type		
$2.35 \times 10^{20} \leqq N_D$	1.04×10^{-6}	0.456
$6.00 \times 10^{19} \leqq N_D \leqq 2.35 \times 10^{20}$	1.43×10^{-12}	0.744
$9.50 \times 10^{18} \leqq N_D \leqq 6.00 \times 10^{19}$	2.00×10^{-16}	0.940
$1.00 \times 10^{17} \leqq N_D \leqq 9.50 \times 10^{18}$	6.93×10^{-9}	0.543
$3.50 \times 10^{15} \leqq N_D \leqq 1.00 \times 10^{17}$	6.97×10^{-14}	0.837
$N_D \leqq 3.50 \times 10^{15}$	2.00×10^{-16}	1.000
p-type		
$1.50 \times 10^{19} \leqq N_A$	4.00×10^{-17}	0.966
$2.40 \times 10^{18} \leqq N_A \leqq 1.50 \times 10^{19}$	1.47×10^{-14}	0.832
$1.50 \times 10^{16} \leqq N_A \leqq 2.40 \times 10^{18}$	3.30×10^{-11}	0.650
$N_A \leqq 1.50 \times 10^{16}$	7.20×10^{-17}	1.000

$C_x = C_s \exp(-x^2/4Dt)$. In these expressions, x, D, and t are the depth, diffusion coefficient (assumed independent of impurity density), and time, respectively. C_x is the concentration of the diffused impurity at depth x and C_s, that at the surface. The former distribution is expected when diffusion takes place with the surface concentration C_s held constant; the latter when the total impurity diffusing is constant. Unfortunately it must be admitted that the accuracy of these expectations is open to question in some situations.[2,16] Also, precipitation and compensation of impurities near the surface may further distort the distribution. However, it is still useful to solve the problem under these assumptions, leaving corrections for later determination.

The "average conductivity" of a diffused layer (which throughout this paper is assumed to be diffused into a silicon slice of opposite conductivity type and uniform doping C_B) is given by the expression

$$\bar{\sigma} = 1/\rho_s x_j = (1/x_j) \int_0^{x_j} q\mu C \, dx$$

where q is electronic charge, μ the carrier mobility typical of a total ionized impurity density of $C_x + C_B$, $C = r(C_x - C_B)$ is the density of carriers, r being the fraction of uncompensated diffused impurity atoms which are ionized, and C_x the total density of diffused impurity atoms at depth x. (Possible variation of the mobility as a function of the proximity of the surface is a hazard which should be recognized in passing but is otherwise ignored in the present calculation.) Multiplying and dividing within the integrand by r' $(C_x + C_B)$, where r' is the ionized fraction associated with an uncompensated dopant density of $(C_x + C_B)$, and writing

$$q\mu r'(C_x + C_B) = \sigma_{(Cx+CB)} = B(C_x + C_B)^{\alpha}$$

the average conductivity becomes

$$\bar{\sigma} = (1/x_j) \int_0^{x_j} (r/r')(C_x - C_B)B(C_x + C_B)^{\alpha-1}\, dx.$$

Now (r/r') represents the ratio of degrees of ionization corresponding to $C_x - C_B$ and $C_x + C_B$ respectively. This ratio is very nearly unity unless C_x and C_B are comparable in magnitude. Such is the case only for the lamina nearest the junction, which contributes negligibly to the conductance of the whole layer. Hence, (r/r') may be justifiably taken as equal to unity, and writing $C_x = C_S f(x)$, where $f(x)$ depends on the profile of interest,

$$\bar{\sigma} = (1/x_j) \int_0^{x_j} [C_S f(x) - C_B]B[C_S f(x) + C_B]^{\alpha-1}\, dx.$$

A program for the evaluation of this expression has been devised previously by others and employed in the analysis of diffused layers in germanium.[17] With slight additions to facilitate automatic plotting, the same program has been used in the present work. Computations were performed on an IBM 704, and plotting of points was carried out with an Electronic Associates Variplotter.

IV. PRESENTATION OF RESULTS

Of frequent interest in transistor design and in the analysis of diffused layers, are the characteristics of a "subsurface" layer such as illustrated in Fig. 2. This layer, bounded on one side by the junction and on the other by a plane paralleling the junction at depth x, may be characterized by an average conductivity

$$\bar{\sigma} = 1/[\rho_S'(x_j - x)] = \frac{1}{(x_j - x)} \int_x^{x_j} q\mu C\, dx$$

where ρ_s' is the sheet resistance of the subsurface layer. It will be recognized that the base region of a diffused-base, alloyed-emitter transistor is an example of a subsurface layer. Another example is that portion of a diffused layer remaining after removing the top strata of depth x. Here, however, it must be remembered that the value of C_s specifying this layer pertains to the original surface at $x = 0$.

Since a subsurface layer becomes the entire diffused layer when $x = 0$, it is convenient to display the properties of both in the same plot by introducing the parameter (x/x_j). On pages 394 to 410 such graphs are presented for n- and p-type diffused layers of Gaussian and complementary error function profile. Each graph contains the family of ten curves $(x/x_j) = 0, 0.1, \cdots, 0.9$, and relates the average conductivity of

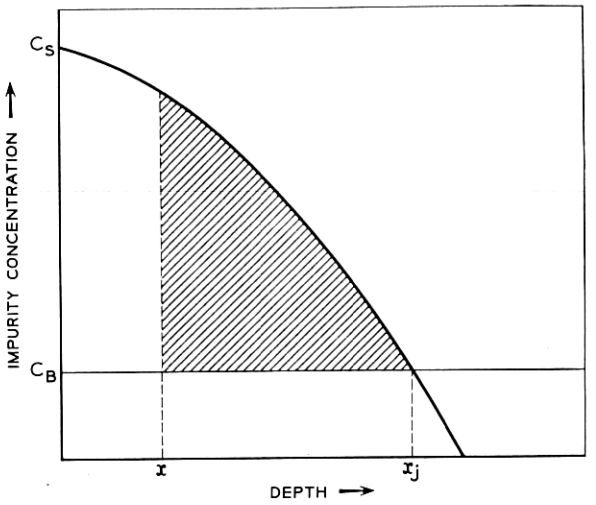

Fig. 2 — Profile of a diffused layer with subsurface layer shaded.

each layer to the surface concentration (at the *original* surface) for a given value of C_B. A separate graph is required for each value of C_B, which in the present work ranges from 10^{14} cm^{-3} to 10^{20} cm^{-3} at one-decade intervals. In each plot the range of surface concentrations spanned is from C_B to 10^{21} cm^{-3}. The so-called "Backenstoss" curve for a particular C_B is simply the right-most line ($x/x_j = 0$) in each graph.

The wiggle in the n-type average conductivity for diffusant concentrations near 10^{19} cm^{-3} is ascribable to the rather large change in slope occurring in the n-type resistivity plot at $N_I = 10^{19}$ cm^{-3}.

V. ACKNOWLEDGMENTS

It is a pleasure to acknowledge the contributions of many colleagues to this investigation. In particular, the boron determinations, devised and performed by C. L. Luke, were very valuable, as were the radioactive arsenic determinations of Miss K. Wolfstirn and Hall-effect measurements of R. A. Logan and R. L. Johnston. The author is indebted to D. Lassota for the growing of the boron-doped crystals, to D. B. Cuttriss, whose efforts brought about the preparation of the computer program, to Mrs. W. Mammel, for subsequent additions to it, to R. Lilienthal for various measurements, and especially to Mrs. M. S. Boyle for her indefatigable assistance in many measurements and the plotting of hundreds of curves.

REFERENCES

1. Backenstoss, G., B.S.T.J., **37**, 1958, p. 699.
2. Tannenbaum, Eileen, Solid-State Electronics, **2**, 1961, p. 123.

3. Backenstoss, G., Phys. Rev., **108,** 1957, p. 416.
4. Carlson, R. O., Phys. Rev., **100,** 1955, p. 1975.
5. Morin, F. J., and Maita, J. P., Phys. Rev., **96,** 1954, p. 28.
6. Ludwig, G. W., and Watters, R. L., Phys. Rev. **101,** 1956, p. 1699.
7. Long, D., Motchenbacher, C. D., and Meyers, J., J. Appl. Phys., **30,** 1959, p. 353.
8. Prince, M. B., Phys. Rev., **93,** 1954, p. 1204.
9. Wolfstirn, K., J. of Phys. & Chem. of Solids, **16,** 1960, p. 279.
10. Logan, R. A., Gilbert, J. F., and Trumbore, F. A., J. Appl. Phys., **32,** 1961, p. 131.
11. Esaki, L., and Miyahara, Y., Solid-State Electronics, **1,** 1960, p. 13.
12. Furukawa, Y., J. Phys. Soc. Japan, **16,** 1961, p. 577.
13. Carlson, R. O., private communication.
14. Luke, C. L., and Flaschen, S. S., Anal. Chem., **30,** 1958, p. 1406.
15. Hatcher, J. T., and Wilcox, L. V., Anal. Chem., **22,** 1950, p. 567.
16. Subashiev, V. K., Landsman, A. P., and Kukharskii, A. A., Soviet Physics-Solid State, **2,** 1961, p. 2406.
17. Cuttriss, D. B., B.S.T.J., **40,** 1961, p. 509.

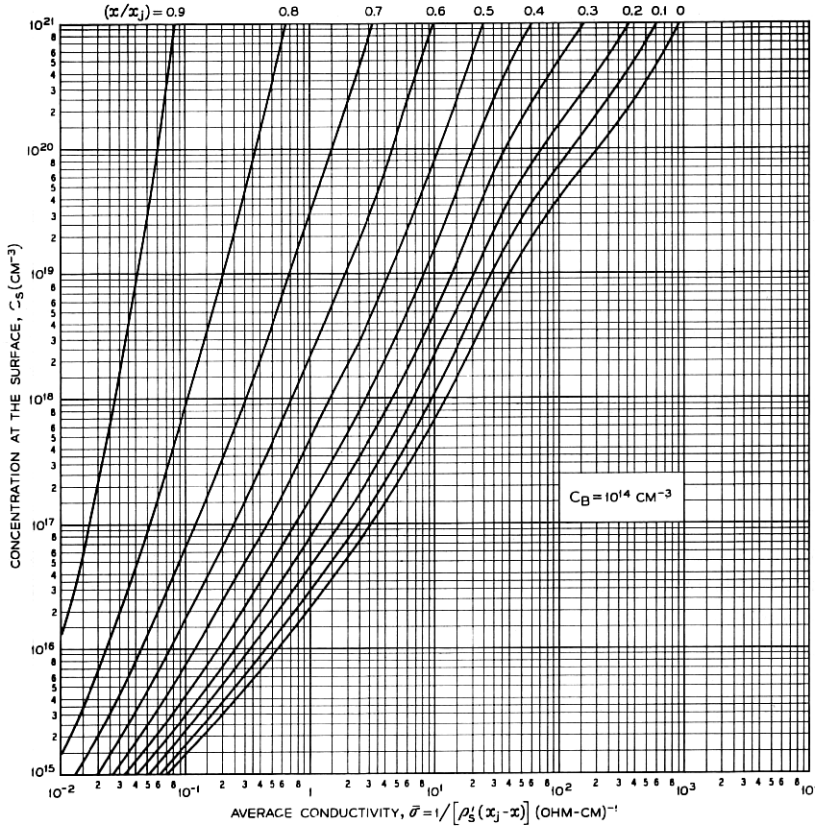

Fig. 3 — Average conductivity of n-type complementary error function layers in silicon.

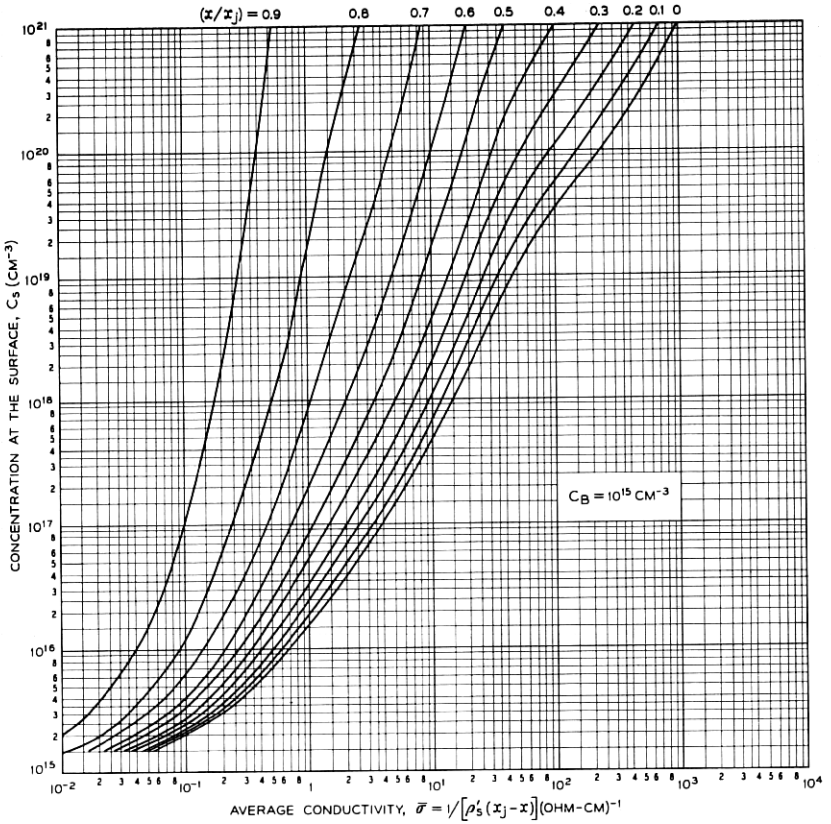

Fig. 3 (cont.) — Average conductivity of n-type complementary error function layers in silicon.

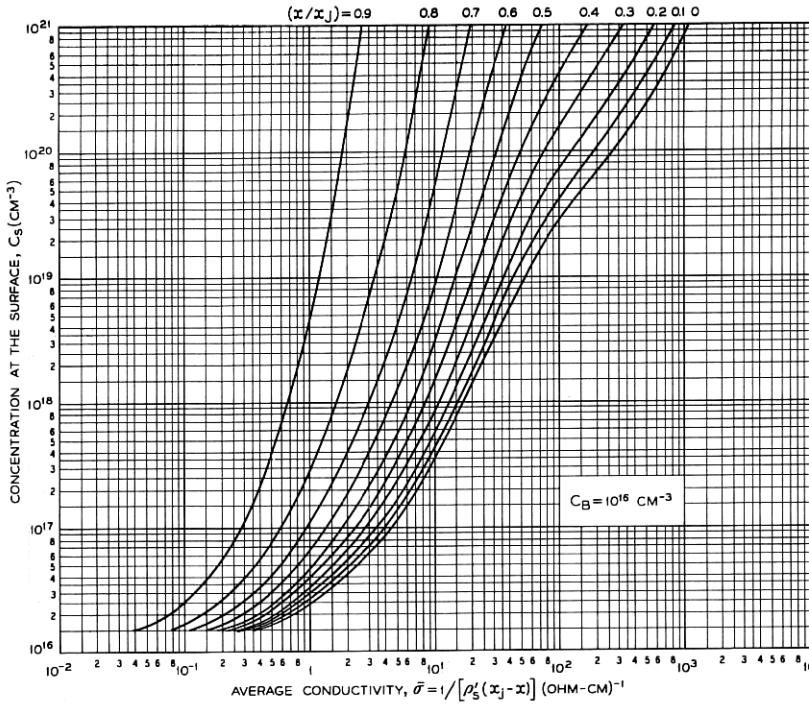

Fig. 3 (cont.) — Average conductivity of n-type complementary error function layers in silicon.

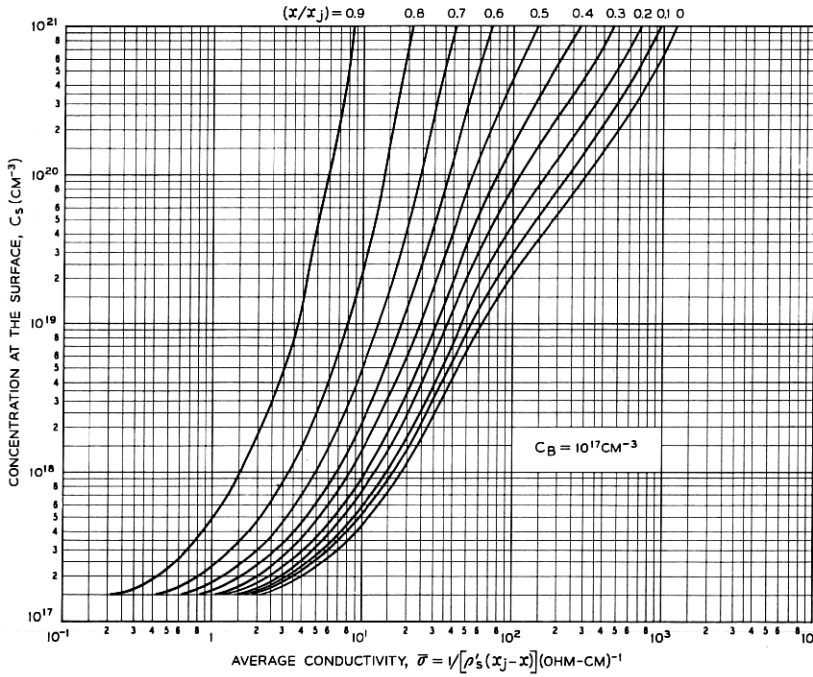

Fig. 3 (cont.) — Average conductivity of n-type complementary error function layers in silicon.

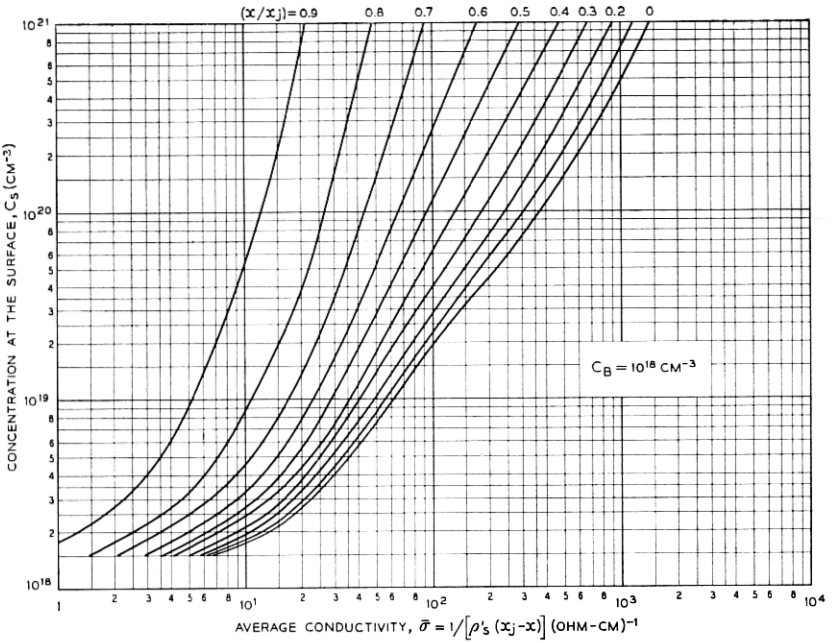

Fig. 3 (cont.) — Average conductivity of n-type complementary error function layers in silicon.

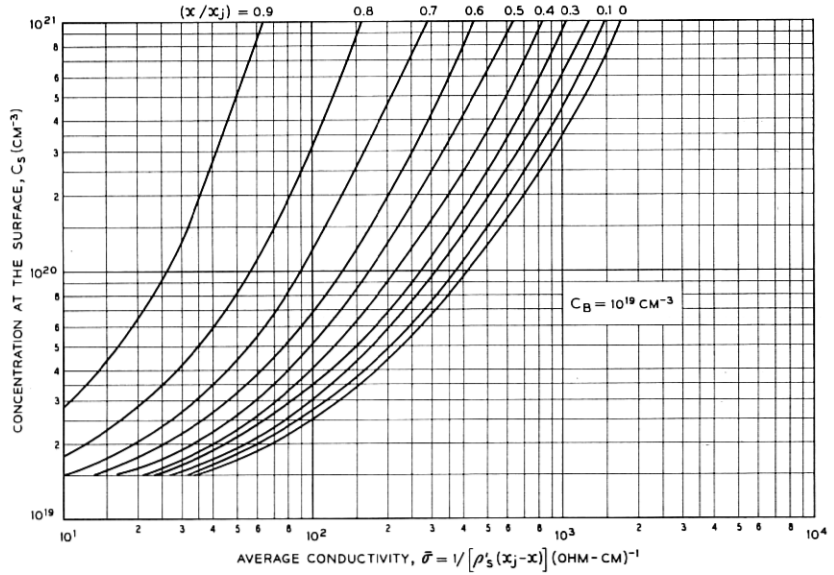

Fig. 3 (cont.) — Average conductivity of n-type complementary error function layers in silicon.

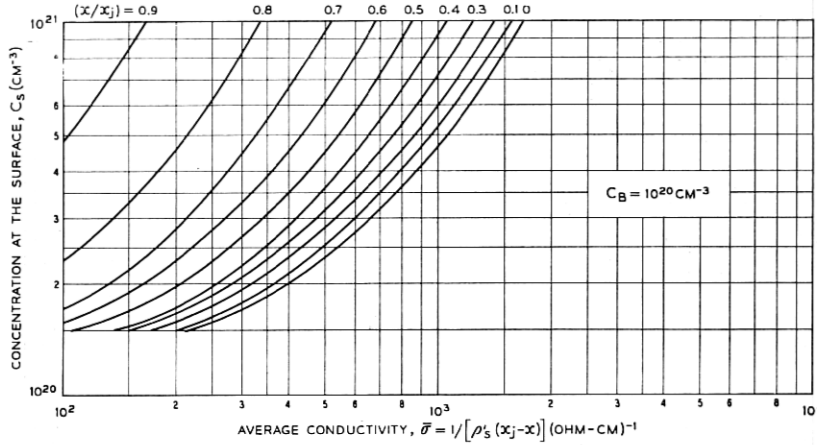

Fig. 3 (cont.) — Average conductivity of n-type complementary error function layers in silicon.

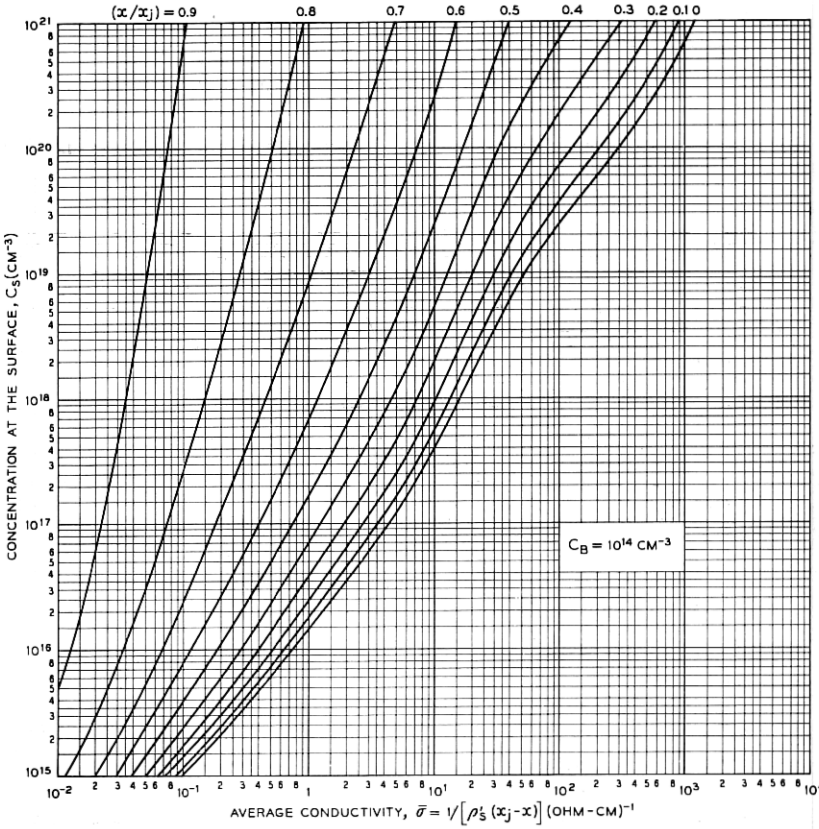

Fig. 4 — Average conductivity of n-type Gaussian layers in silicon.

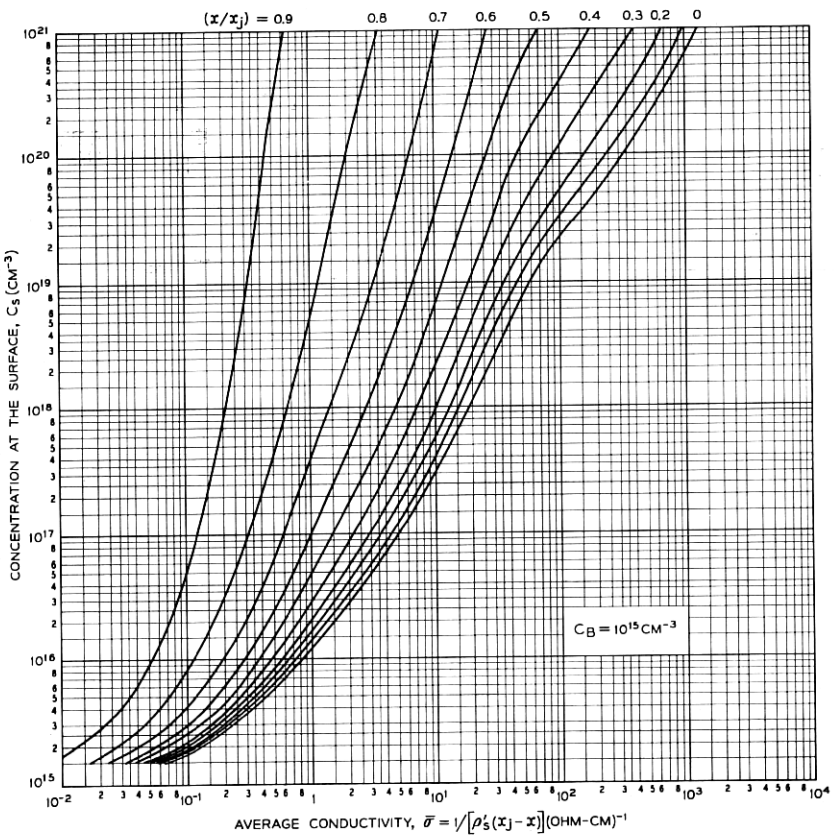

Fig. 4 (cont.) — Average conductivity of n-type Gaussian layers in silicon.

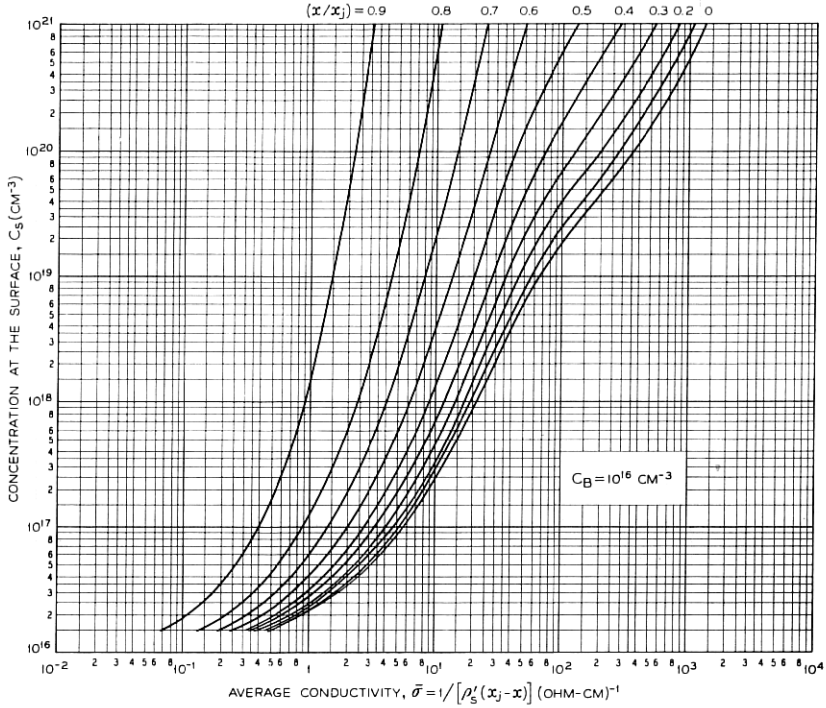

Fig. 4 (cont.) — Average conductivity of n-type Gaussian layers in silicon.

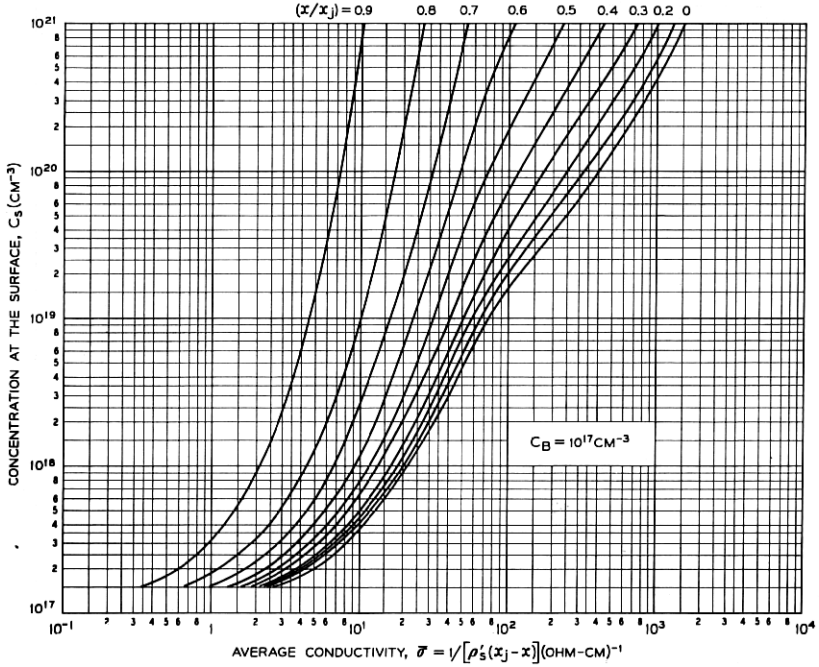

Fig. 4 (cont.) — Average conductivity of n-type Gaussian layers in silicon.

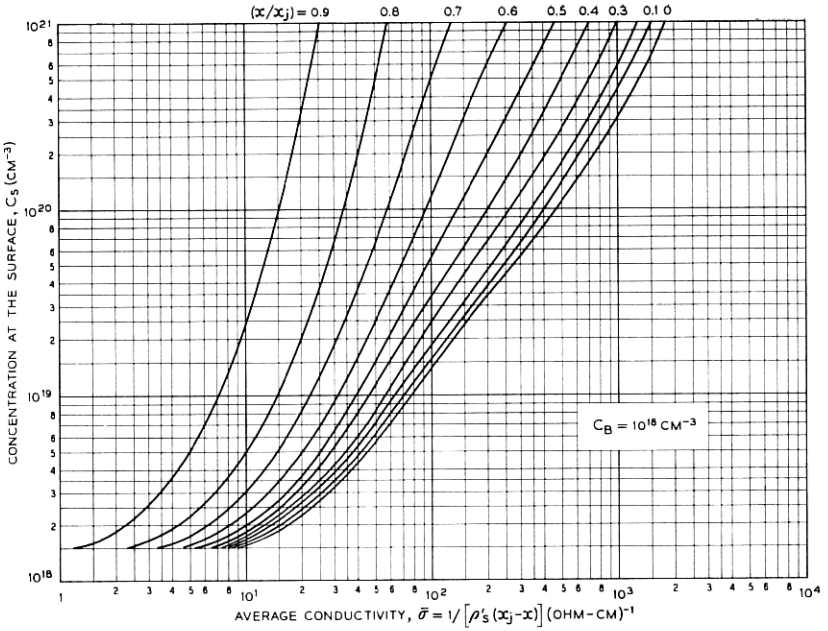

Fig. 4 (cont.) — Average conductivity of n-type Gaussian layers in silicon.

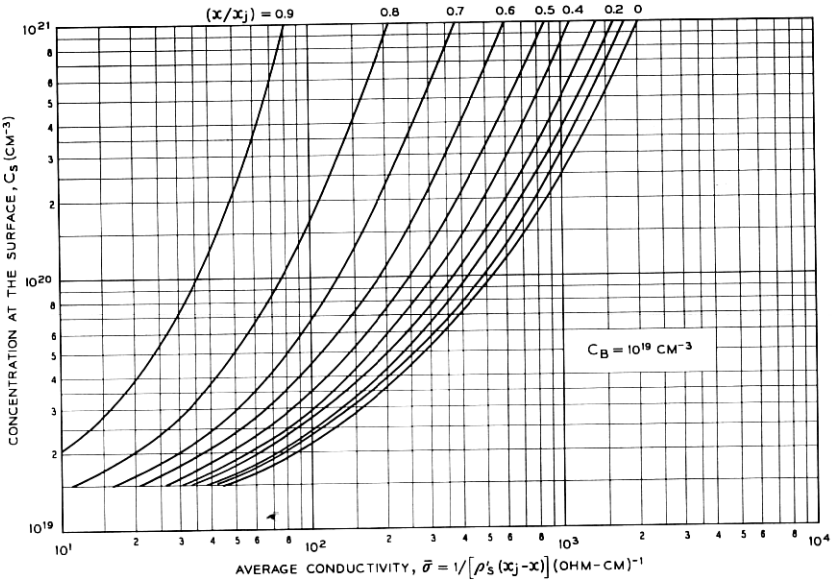

Fig. 4 (cont.) — Average conductivity of n-type Gaussian layers in silicon.

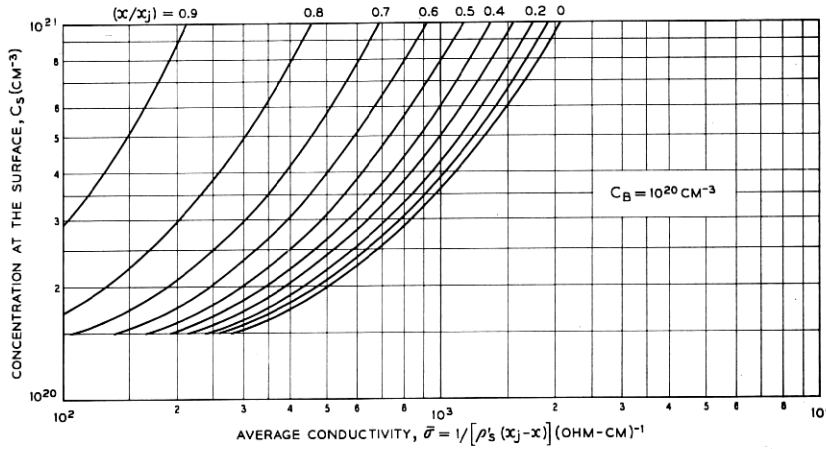

Fig. 4 (cont.) — Average conductivity of n-type Gaussian layers in silicon.

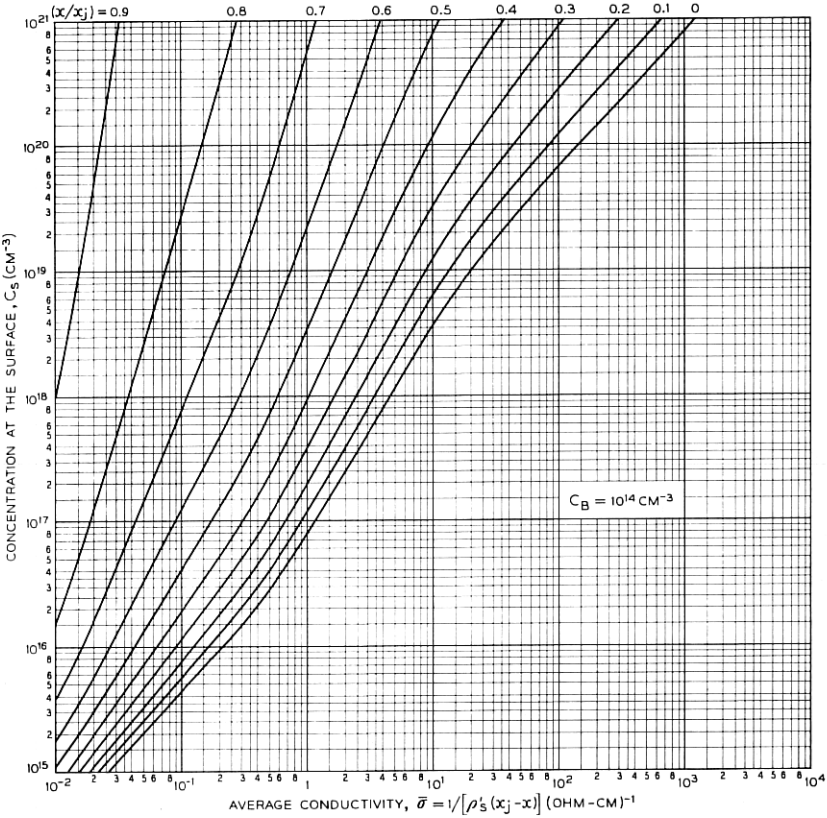

Fig. 5 — Average conductivity of p-type complementary error function layers in silicon.

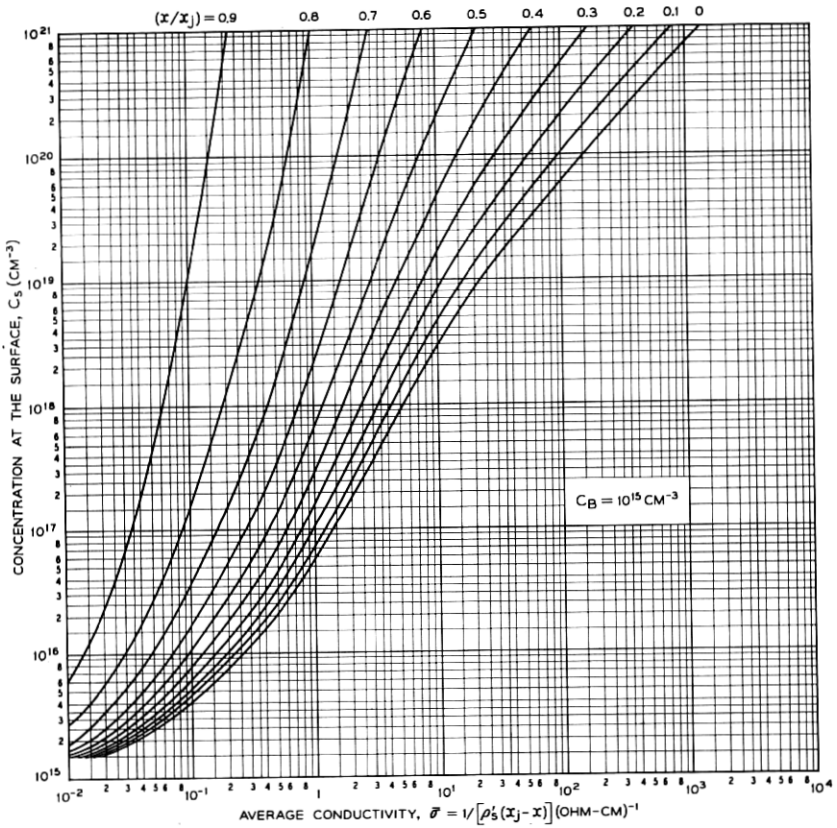

Fig. 5 (cont.) — Average conductivity of p-type complementary error function layers in silicon.

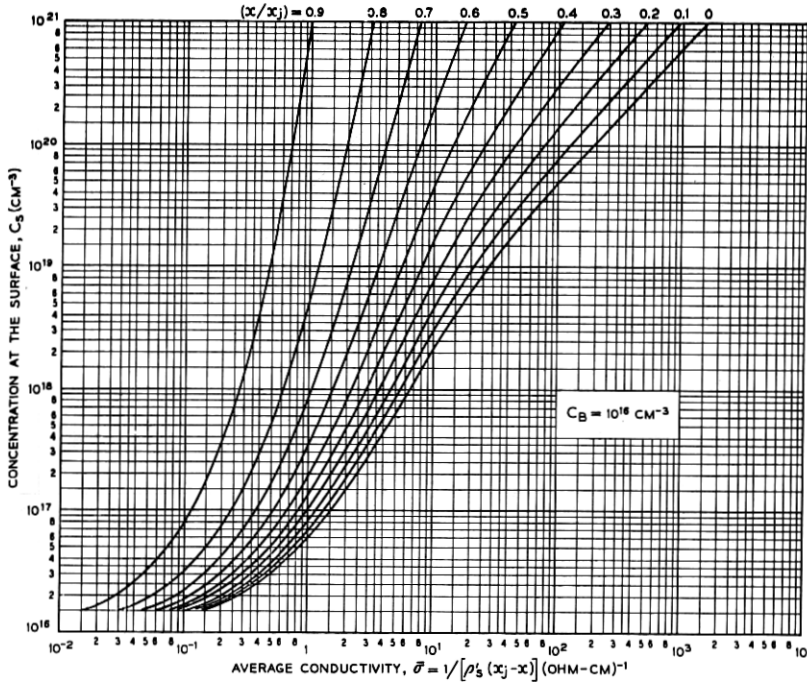

Fig. 5 (cont.) — Average conductivity of p-type complementary error function layers in silicon.

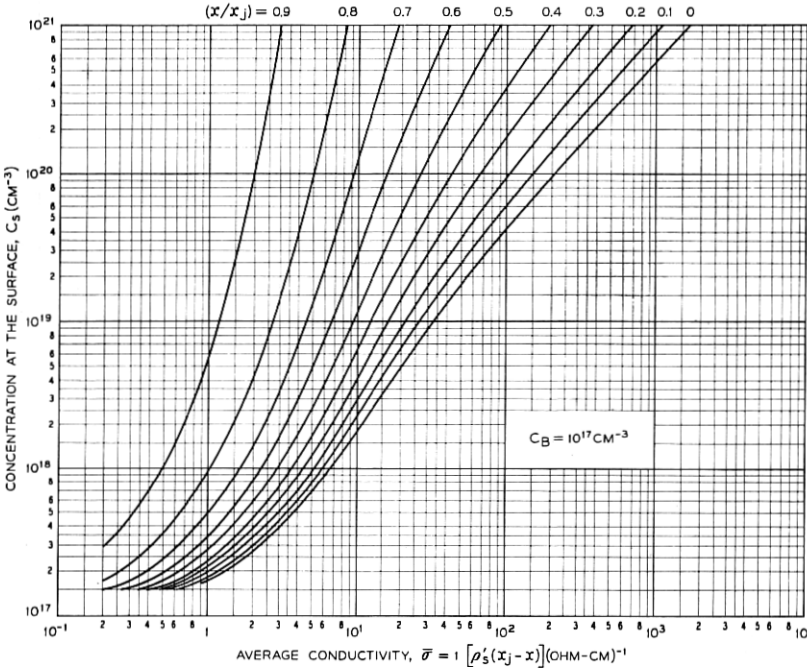

Fig. 5 (cont.) — Average conductivity of p-type complementary error function layers in silicon.

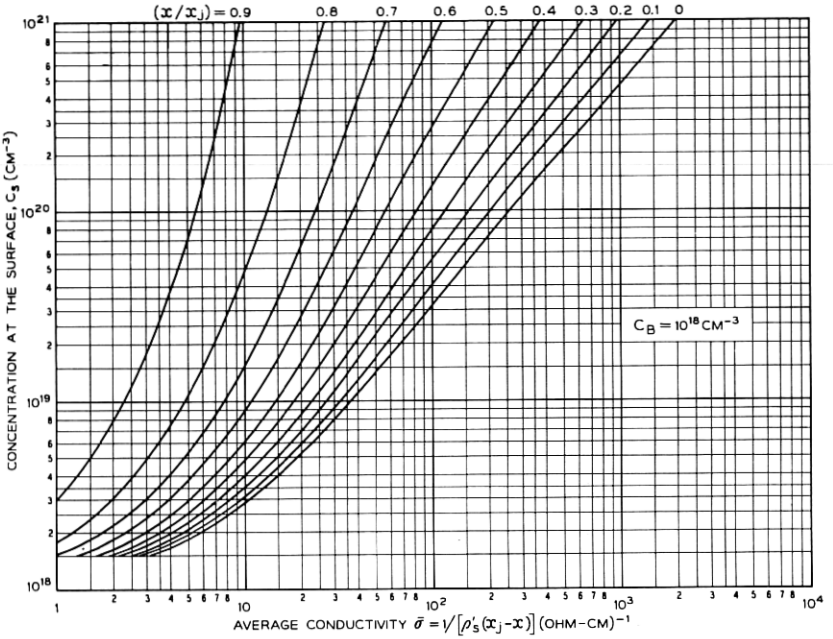

Fig. 5 (cont.) — Average conductivity of p-type complementary error function layers in silicon.

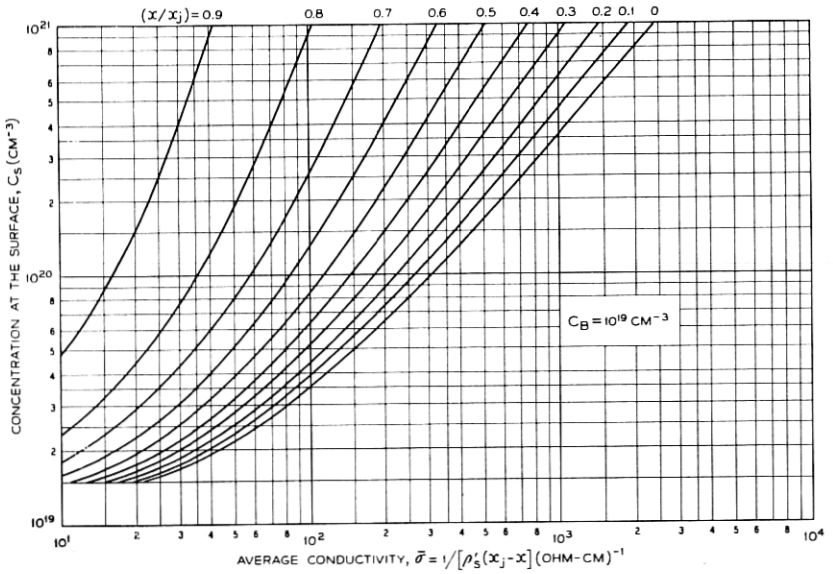

Fig. 5 (cont.) — Average conductivity of p-type complementary error function layers in silicon.

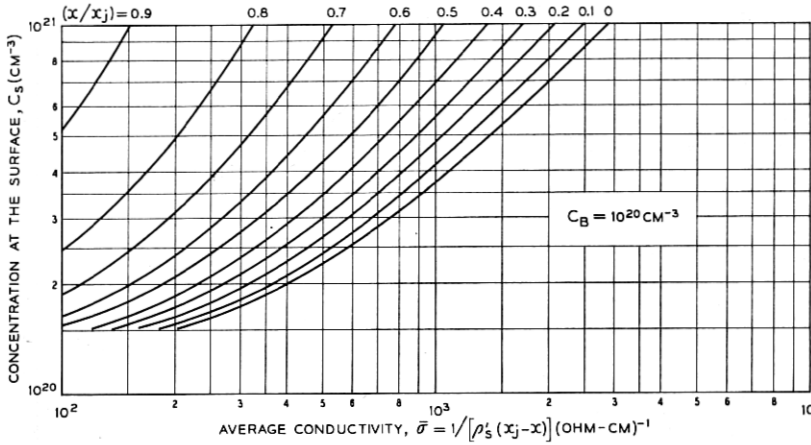

Fig. 5 (cont.) — Average conductivity of p-type complementary error function layers in silicon.

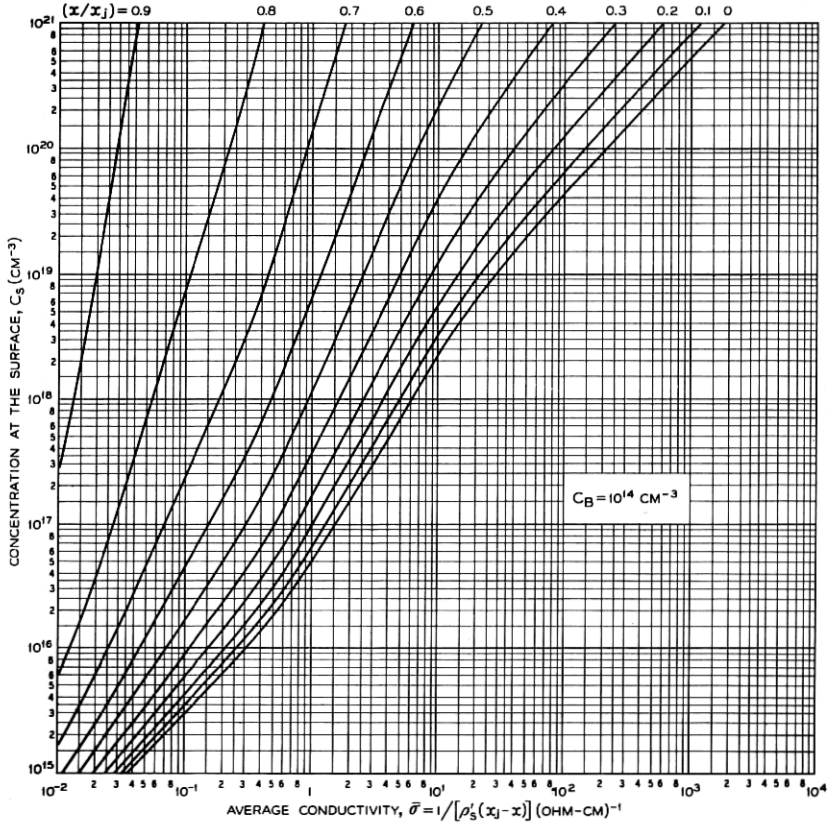

Fig. 6 — Average conductivity of p-type Gaussian layers in silicon.

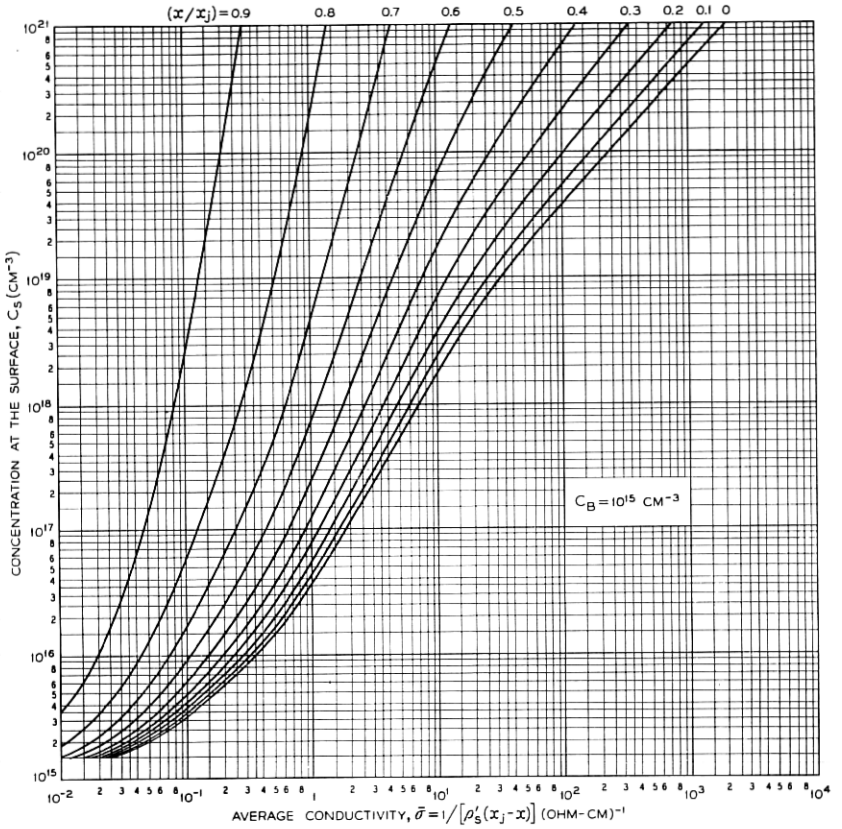

Fig. 6 (cont.) — Average conductivity of p-type Gaussian layers in silicon.

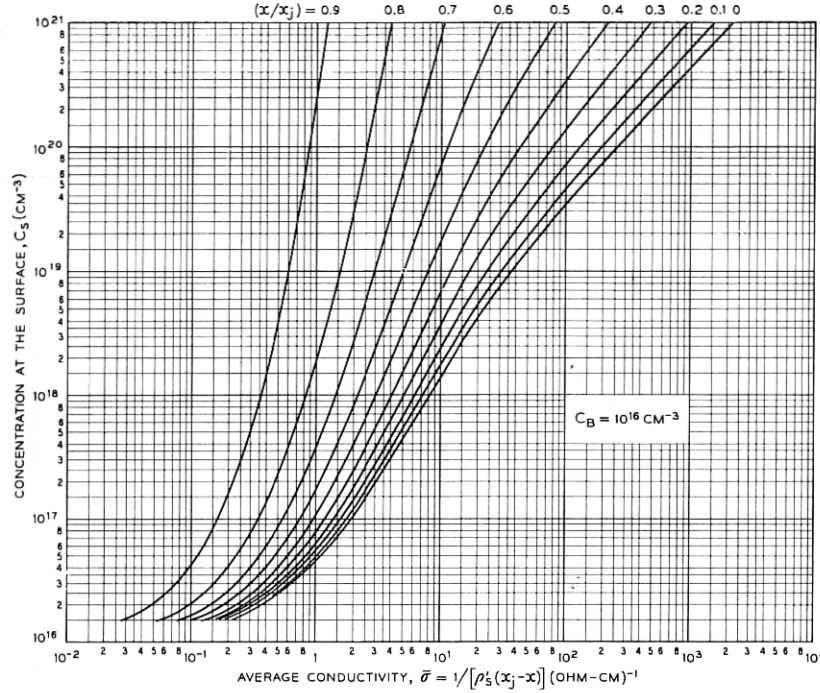

Fig. 6 (cont.) — Average conductivity of p-type Gaussian layers in silicon.

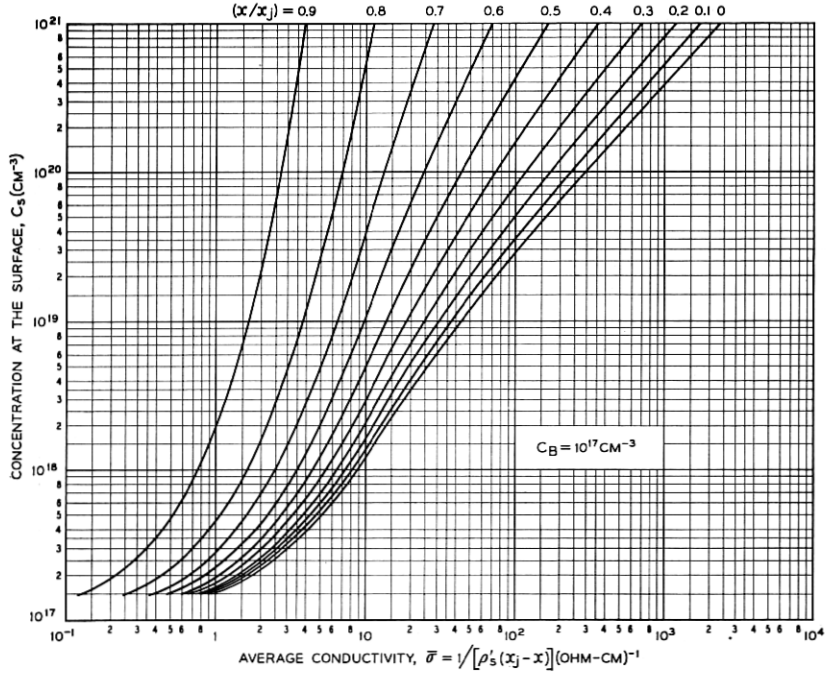

Fig. 6 (cont.) — Average conductivity of p-type Gaussian layers in silicon.

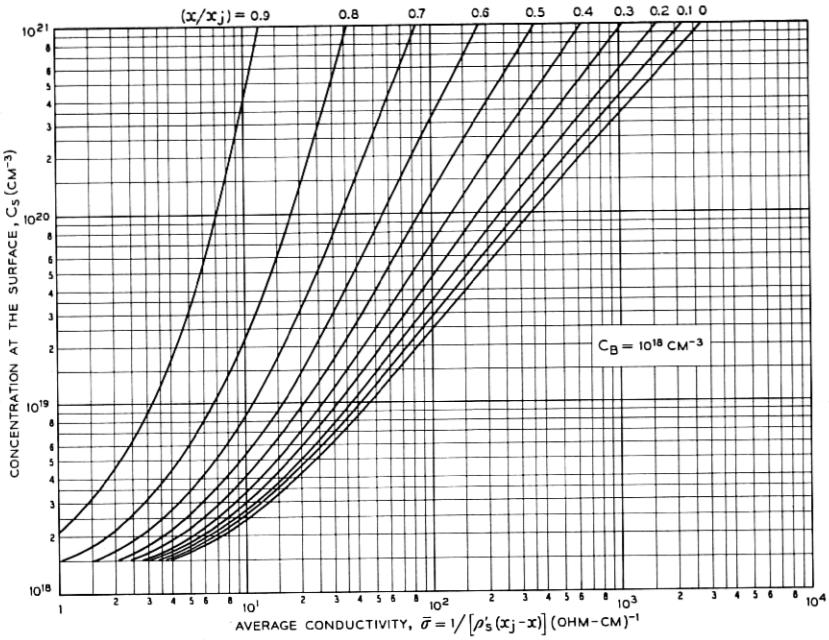

Fig. 6 (cont.) — Average conductivity of p-type Gaussian layers in silicon.

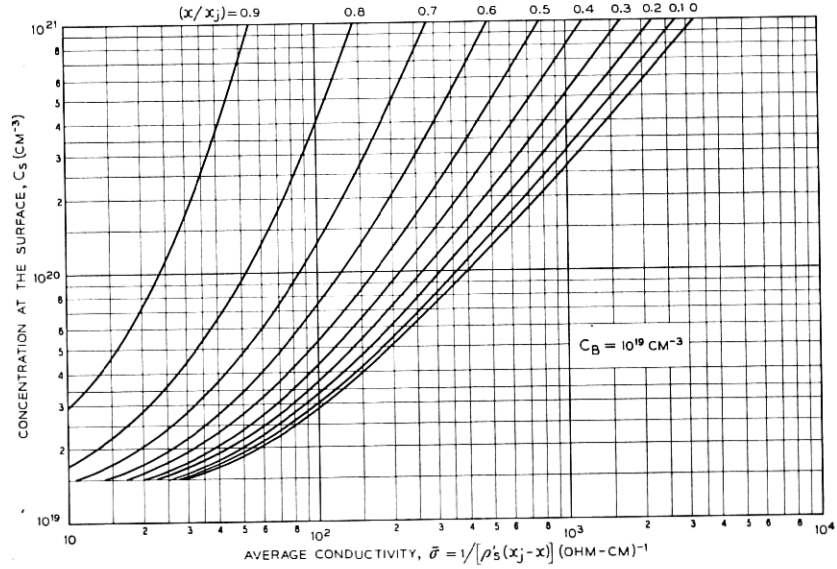

Fig. 6 (cont.) — Average conductivity of p-type Gaussian layers in silicon.

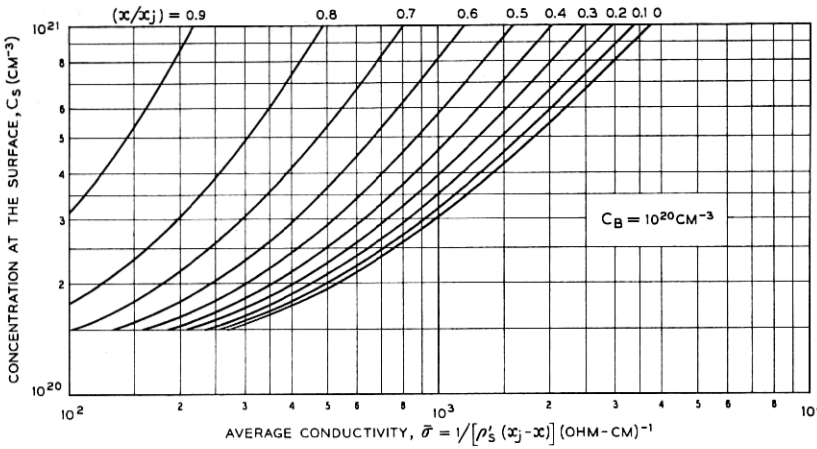

Fig. 6 (cont.) — Average conductivity of p-type Gaussian layers in silicon.